

Crystal Plasticity Analysis of Ridging in 6000 Series Alloys

Haruyuki Konishi¹, Katsushi Matsumoto², Yasuo Takaki³, Yasuhiro Aruga²,

¹Aluminum & Copper Company, KOBE STEEL, 1-5-5 Takatsukadai, Nishi-ku, Kobe, Hyogo 651-2271, Japan

²Materials Research Laboratory, KOBE STEEL, 1-5-5 Takatsukadai, Nishi-ku, Kobe, Hyogo 651-2271, Japan

³Aluminum & Copper Company, KOBE STEEL, 15 Kinugaoka, Moka, Tochigi 321-4367, Japan

Crystal plasticity analysis in 6000 series alloy sheet was performed to clarify the origin of ridging formation. The formulation of rate dependent crystal plasticity was used in finite element analysis. Crystallographic orientation distribution of the alloy which showed serious ridging was measured by SEM/EBSD technique. Surface deformations of the alloy under stretching were numerically predicted based on the orientation distribution measured.

In the numerical results, large curves of the sheet plane were predicted, and it was considered that these curves characterized ridging behavior of the alloy. In the cross sections of the alloy sheet, large area of cube grains and Goss grains distributed inhomogeneously were observed. From the numerical results, it was thought that these inhomogeneous distributions of cube and Goss grains caused the non-symmetric deformation property, and the sheet showed out-of-plane deformation (curve) during stretching. And these distributions of cube and Goss grains were supposed as an origin of ridging.

Keywords: 6000 series alloy, Ridging, Texture, Crystal Plasticity

1. Introduction

6000 series alloys have excellent properties for the car body parts, such as high strength after baking treatment, sufficient formability and good corrosion resistance. From these advantages, the application of these alloys to closure panel was thought as an effective solution for the needs of weight reduction of car body.

However, on the sheet surface after stamping, banded surface defects called ridging (or roping) are sometimes formed, and it is an important issue for the application of these alloys. There have been many studies on the ridging of 6000 series alloy[1-4], and it was reported that banded structure of cube grains or Goss grains which are aligned parallel with rolling direction(RD) caused ridging. However, the details of the mechanism have not been clear enough because of the difficulties in evaluating the effect of plastic anisotropy of these oriented grains, which are spatially distributed in the bulk and could be the origin of a ridging.

Crystal plasticity analysis would make us possible to estimate these effects. Especially by combining with electron backscatter diffraction (EBSD) technique in scanning electron microscope (SEM), this approach allows us to understand the relationship between the actual banded surface topography and the arrangement of texture components through the thickness.

In this study, ridging behavior of two types of sheet alloy which was prepared by different heat treatment was investigated. Surface deformation of these alloys after stretching was measured to evaluate ridging. Then crystal orientation distribution was measured by SEM/EBSD technique, and poly-crystal models for the numerical analysis were made. And crystal plasticity analysis was performed based on the poly-crystal models. In the result, deformation behavior of ridging-prone alloy was characterized by curving. And several mechanisms of the ridging were proposed based on several numerical results.

2. Experimental analysis

2.1 Experimental procedure

A hot rolled strip having chemical composition of 6111 was used in this study. The hot rolled strip was annealed, cold rolled and solutionized under the condition shown in Table 1, and two types of samples A, B of T4 temper with different conditions of intermediate annealing having 1.0mm thickness were made.

Crystallographic orientation distribution on a cross section perpendicular to RD was measured by EBSD system (TSL, Orientation Imaging Microscopy(OIM)) attached to a scanning electron microscope.

Specimens for tensile test with $40 \times 150 \times 1 \text{ mm}^3$ in size were cut out from each samples, and the specimens were stretched 15% in transverse direction. After the tensile tests, surface profiles of the specimens were measured by contour measurement contracer (MITSUTOYO CDH-400).

Table 1 Conditions of heat treatment and rolling

Sample	Intermediate annealing	cold rolling	Solution treatment
A	500°C × 10s (salt bath)	1.0mmt	550°C × 1min (batch type furnace) → Water Quench
B	350°C × 3hr (batch type furnace)		

2.2 Experimental result

Crystallographic orientation map of each sample are shown in Fig.1 with the area fraction of typical crystal orientation components in the section. The area fraction was calculated for grains with a deviation of less than 15° from an exact orientation respectively. Sample-A has relatively random texture. The grains of Sample-A is equiaxed shape, and its average grain size is 32 μm. On the other hand, Sample-B shows evolution of cube, ND-cube, S and Goss orientation components. Grain shape of Sample-B is relatively elongated to transverse direction (TD). Cube grains were distributed inhomogeneously near the surface layer. Goss grains were also distributed in the section.

Surface appearance after 15% stretching for each sample are shown in Fig.2. In the case of Sample-B, small valley and ridge parallel to rolling direction were observed. In the case of Sample-A, few valley or ridge were observed, and Sample-A seemed to have better quality for ridging than Sample-B.

Surface profiles after 15% stretching for each sample are shown in Fig.3. Measurement was performed along the four lines parallel to and 1mm apart from each other. In the case of Sample-B, wavy displacement about 5 μm of amplitude and 2-3mm cycle are observed, and the coincidence is found in the position of peaks and valleys in adjacent lines of measurement. Thus, the surface displacement is considered banded structure.

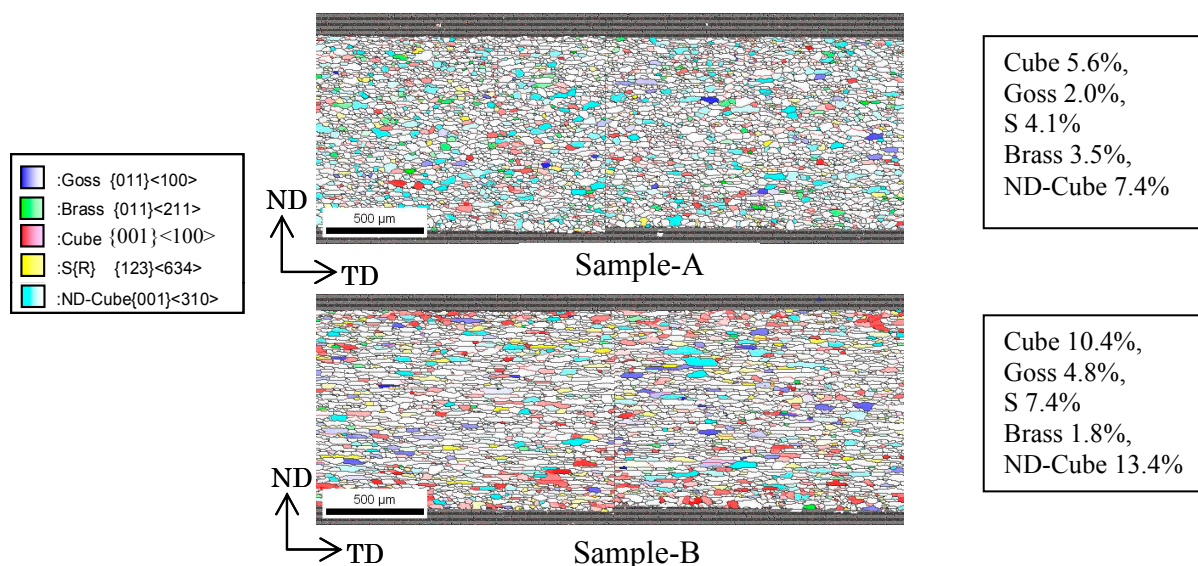


Fig. 1 SEM/EBSD maps of tested samples

In the case of Sample-A, surface displacement with the amplitude about $3 \mu\text{m}$ are found on each base line. However, the tendency of the coincidence of peak and valley positions in adjacent lines is not so clear, and the surface displacement in Sample-A is considered not to form apparent banded structure. From these result, it was concluded that ridging behavior appeared in the surface of Sample-B was caused by ridge and valley displacement parallel with rolling direction and its depth is about $5 \mu\text{m}$ and wave length is about 2-3mm. The occurrence of similar crystals orientation distribution in adjacent section in RD was considered to have caused such ridge or valley.

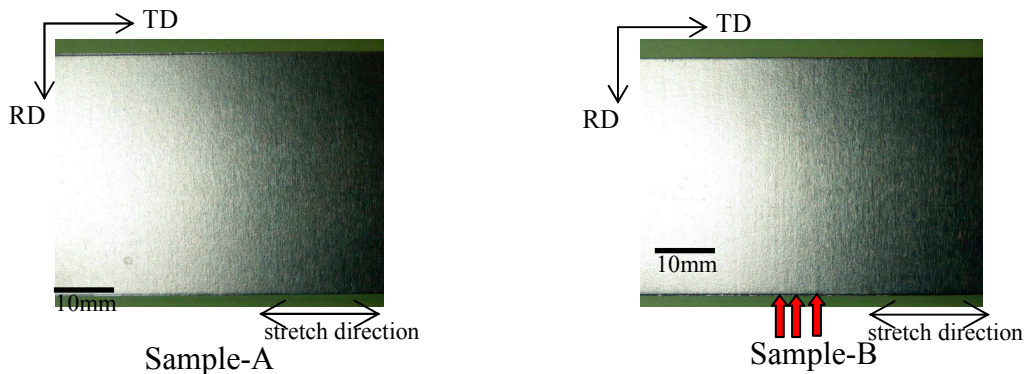


Fig.2 Surface appearance after 15% stretch

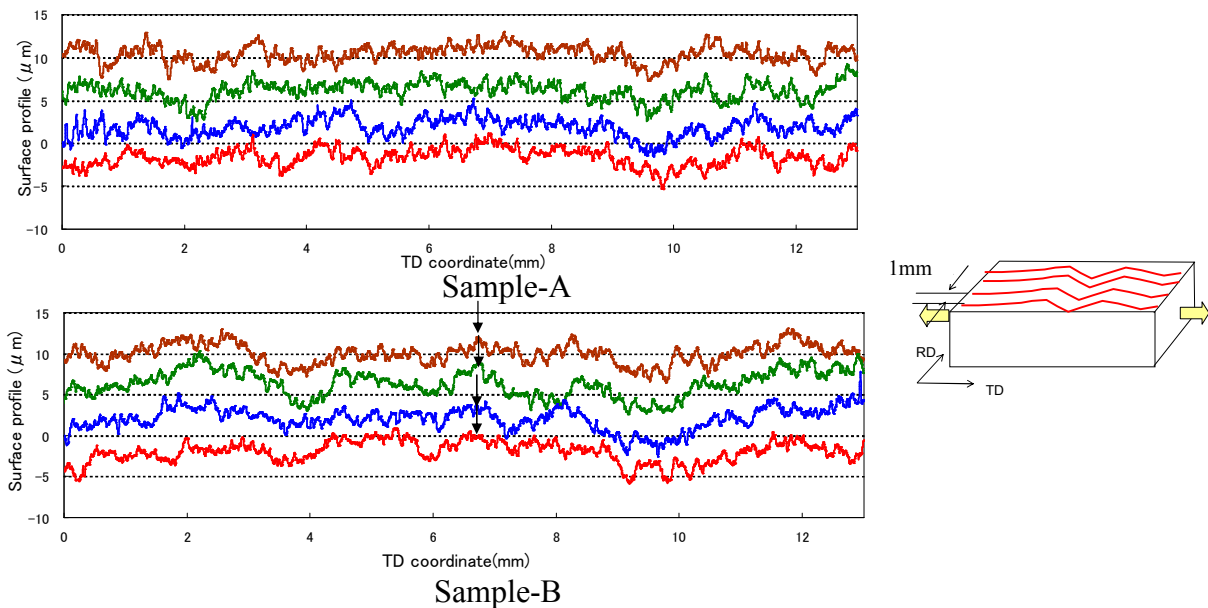


Fig.3 Surface profile of each sample after 15% stretch
(Base lines for each profile were shifted upward by $5 \mu\text{m}$)

3. Crystal plasticity analysis of ridging

3.1 Constitutive equation and numerical analysis model

Rate dependent crystal plasticity theory proposed by Peirce et al [5], which can evaluate the influence of crystallographic texture on deformation property was implemented in FEM analysis code and deformation analysis were performed [6]. The summary of the theory is shown below.

Crystal slip caused by the resolved shear stress is considered. The power-law relation between slip rate $\dot{\gamma}^{(\alpha)}$ and resolved shear stress $\tau^{(\alpha)}$ on slip system α is assumed as follows.

$$\dot{\gamma} = \dot{a}^{(\alpha)} \left(\frac{\tau^{(\alpha)}}{g^{(\alpha)}} \right) \left| \frac{\tau^{(\alpha)}}{g^{(\alpha)}} \right|^{1/m-1} \quad (1)$$

Introducing Eq. (1) into the kinematical equation concerning plastic deformation due to crystal slip, the following relation of stress rate expressed deformation rate is obtained,

$$\dot{\tilde{T}} \equiv \dot{T} + T \text{tr} d = L^e d - \sum_{\alpha=1}^n R^{(\alpha)} \dot{\gamma}^{(\alpha)} \quad (2)$$

where T , \dot{T} , L^e means Cauchy stress, its Jaumann rate and elastic modulus respectively. $R^{(\alpha)}$ is the second order tensor calculated by lattice rotation and stress, n is number of slip system. The value $g^{(\alpha)}$ in Eq. (1) which expresses current hardening state is assumed to follow self hardening and latent hardening law. Thus the increase rate of $g^{(\alpha)}$ may be expressed by,

$$\dot{g}^{(\alpha)} = \sum h_{\alpha\beta} |\dot{\gamma}^{(\beta)}| \quad (3)$$

And hardening modulus $h_{\alpha\beta}$ is presumed to be specified by the following equations.

$$h_{\alpha\beta} = qH + (1-q)H\delta_{\alpha\beta} \quad , \quad H(\gamma) = \frac{d\tau(\gamma)}{d\gamma} \quad , \quad \gamma = \sum_{\alpha=1}^n |\gamma^{(\alpha)}| \quad (4), (5), (6)$$

q is the ratio of latent hardening to self hardening.

Crystal structure of fcc are considered and following material properties were used in the analysis.

- Elastic properties : $E = 70$ GPa, $\nu = 0.3$
- Hardening properties: $\tau = \tau_0 + (\tau_s - \tau_0) \tanh\left(\frac{H_0 \gamma}{\tau_s - \tau_0}\right)$, $\tau_0 = 47.5$ MPa, $\tau_s = 107.8$ MPa, $H_0 = 168.8$ MPa, $q = 1$, $n = 12$
- Material rate sensitivity: $m = 0.005$

Cross sections of the two samples shown in Fig.1 were chosen as the region of numerical analysis. The areas were modeled 70×170 finite element mesh, and crystal orientation was assigned for each element by using the information of the orientation map. Tensile deformation into transverse direction under plane strain condition was numerically analyzed.

3.2 Crystal plasticity analysis results

Deformed section of each samples are shown in Fig.4 (a)(b). In these figures, displacement normal to the sheet plane is enlarged 10time to evaluate deformation mode more clearly. Both material show curving and fluctuation of thickness, but the curving of Sample-B seems to be more remarkable. The relationship between amount of curving, fluctuation of thickness and tensile strain are shown in Fig.5. Here, the amount of curving was defined as the out of plane displacement of center line of each section. Fluctuation of thickness was defined as the difference between maximum thickness and minimum thickness. The fluctuation of the thickness of Sample-B doesn't differ much with Sample-A, so it was supposed that the fluctuation of thickness does not reflect specific ridging behavior of each sample. On the other hand, the curving of Sample-B shows larger value than Sample-A. Thus we presumed that the amount of curving express the level of ridging. In other words, we presumed that ridging-prone Sample-B exhibits larger curving deformation when it is subjected to stretching, and the curving deformation was recognized as the ridge and valley on the surface.

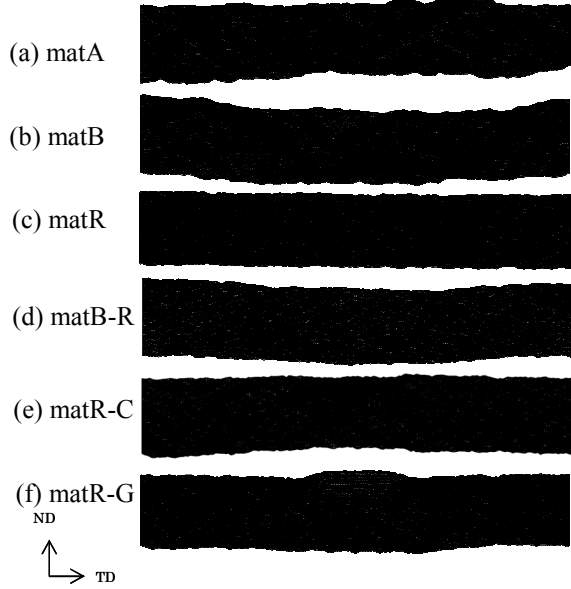


Fig.4 Deformed section shape predicted by crystal plasticity analysis of each material
(After 5% stretch, out of plane displacement was enlarged 10 times)

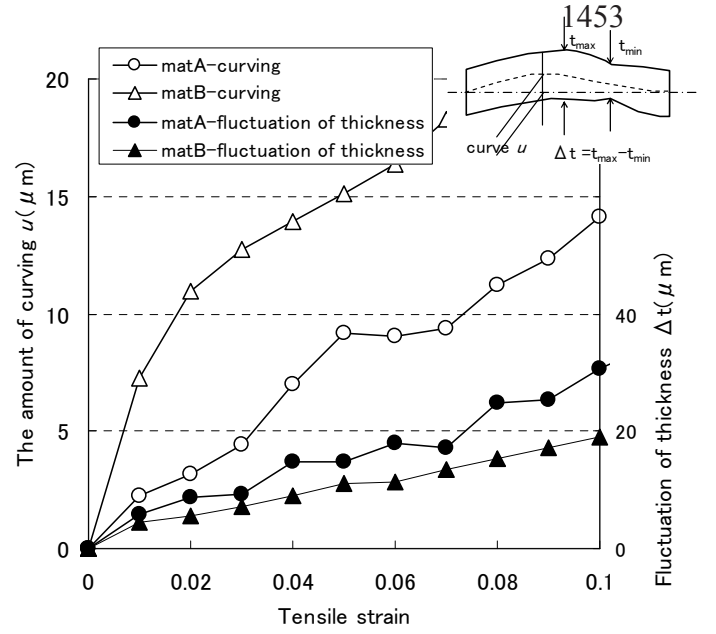


Fig.5 The relationship between curving, fluctuation of thickness and tensile strain

4. Extensive numerical analysis to study the mechanism of ridging

In the previous section, we presumed that the difference of ridging behavior between two samples was caused by the nature of curving. To study the mechanism of the curving, we performed additional numerical analysis.

Conditions of additional numerical analysis are shown in Table 2. MatR is the case of ideal crystal with random orientation where the orientation distribution function is distributed uniformly in Euler space, and spatial distribution of the grains of each orientation is also random. Volume fraction of the grain which has an orientation $(\varphi_1, \Phi, \varphi_2)$ is determined by following equation [7].

$$\frac{V^{(i)}}{V} = \int_{\varphi_1}^{\varphi_1+d\varphi_1} \int_{\Phi}^{\Phi+d\Phi} \int_{\varphi_2}^{\varphi_2+d\varphi_2} \frac{\sin \Phi}{8\pi^2} d\varphi_1 d\Phi d\varphi_2 \quad (7)$$

MatR-C, matR-G are the cases, where square area of cube or Goss orientation was embedded in the region of random material matR. The square area has the size of $600 \mu\text{m} \times 114 \mu\text{m}$, and is located near the one side of the surface. MatB-R is the case where its over all crystal orientation distribution is the same with that of mat(Sample-B), but the arrangement of the grains in matB was randomized.

Deformed section shapes of each case are shown in Fig.4(c)~(f), and the out of plane displacement of the center line of the region are shown in Fig.6. In the case of matR, both the curve of the section and the fluctuation of thickness are very small, and macroscopically uniform deformation is observed. On the other hand, in the case of matB-R, both the curve and the fluctuation of thickness are smaller than matB, but the slight curve is still observed.

In the case of matR-C, curving deformation toward upward is observed. And it is also found that, the thickness of the section where the cube area was embedded is smaller than other. On the other hand, in the case of matR-G, curving tendency to downward is observed, and the thickness of the section where the Goss area was embedded, is larger than other.

Plastic flow stresses of single crystal having various orientations were numerically analyzed. Tensile stress-strain relations in transverse direction under plane strain condition are shown in Fig.7. It is found that the flow stress for cube orientation is smaller, and the flow stress for Goss orientation is larger than those of other orientations. Such difference of flow stress in these orientations was considered to have caused the fluctuation of the thickness in matR-C and matR-G. And it is also considered that the harder or softer area embedded in the random area made the stress distribution non-uniform, and consequently curve deformation was caused in these materials.

For the curving deformation observed in matB-R, there may be some other mechanisms to explain the reason. Further study is necessary to solve the problem.

5. Conclusion

Mechanism of ridging behavior of 6000 series Al sheet alloy was studied by crystal plasticity analysis based on the results of SEM/EBSD measurement. The following conclusion was obtained.

- The ridging behavior in Sample-B was characterized by large curve of the sheet.
- Inhomogeneous distribution of cube or Goss grains was considered to be a reason for curve. Such distributions make stress flow non-uniform in the section, and cause curve of the sheet.

Table 2 Conditions of deformation analysis

CASE	Crystal orientation	
matA	Sample-A	
matB	Sample-B	
matR	Ideal random orientation material	
matB-R	Arrangement of grains of mat-B was randomized	
matR-C	Cube area is added into matR	
matR-G	Goss area is added into matR	

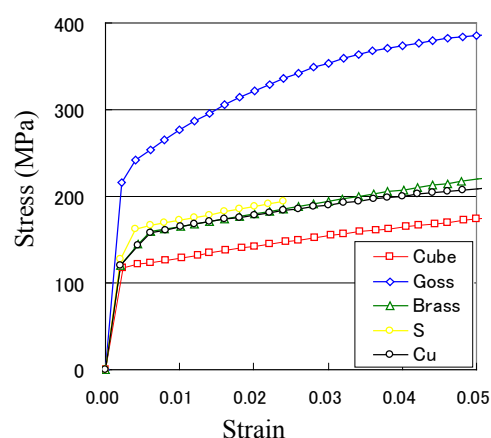


Fig. 7 Stress-strain relation of single crystal of various crystal orientation in transvers direction stretching

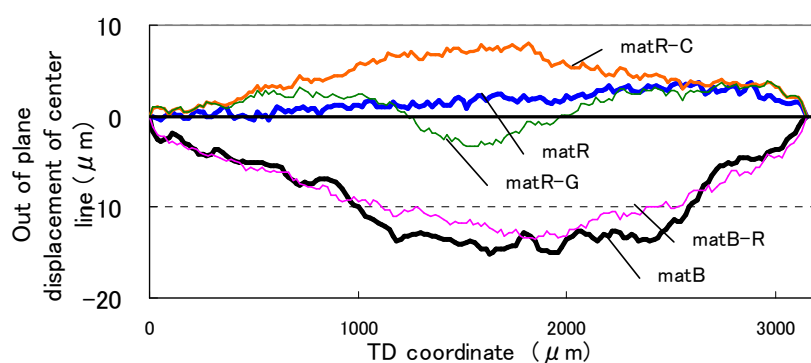


Fig. 6 Predicted out of plane displacement of center line of the area

References

- [1] A. J. Beaudoin, J.D.Bryant and D.A. Korzekwa: Metall. Mater. Trans. A. 29A (1998), p2323-2332.
- [2] H. Jin, P.D. Wu, M. D. Ball, D.J.Lloyd, Material Science and Technology, 21-4(2005), p419-428.
- [3] H. Jin, D.J.Lloyd, Material Science and Engineering, 403(2005), p112-119.
- [4] D.Raabe, M.Sachtleber, H. Weiland, G. Scheele, and Z. Zhao, Acta Mater. 51(2003),p1539-1560
- [5] D.Peirce, J.Asaro, A. Needleman, Acta Met. 31-12(1983),p1951-1960.
- [6] H. Kitagawa, A. Nakatani and H. Konishi: Proceeding ICES95, (1995), p2093-2098.
- [7] H.J. Bunge: *Texture analysis in Materials Science*, 3. Aufl., 2. Bd., (Butterworths, 1982) .